Research · Science
Forschung · Wissenschaft
Recherche · Science

Articles published in this section have been reviewed by members of the Editorial Review Board.

Jede im SDJ eingereichte Arbeit wird von zahnärztlichen Fachpersonen begutachtet. Diese genaue Begutachtung macht es möglich, dass die Publikationen einen hohen wissenschaftlichen Standard aufweisen.

Ich bedanke mich bei den unten aufgeführten Kolleginnen und Kollegen für ihre wertvolle Mitarbeit, die sie in den vergangenen drei Jahren geleistet haben.

Adrian Lussi

Thomas von Arx[1,2]
Scott Lozanoff[2]

[1] Department of Oral Surgery and Stomatology, School of Dental Medicine, University of Bern, Bern, Switzerland
[2] Department of Anatomy, Biochemistry and Physiology, John A. Burns School of Medicine, University of Hawaii, Honolulu, HI/USA

CORRESPONDENCE
Prof. Dr. Thomas von Arx
Department of Oral Surgery and Stomatology, School of Dental Medicine, University of Bern
Freiburgstrasse 7
CH-3010 Bern, Switzerland
Tel. +41 31 632 25 66
Fax +41 31 632 25 03
E-mail:
thomas.vonarx@zmk.unibe.ch

SWISS DENTAL JOURNAL SSO 125: 1202–1209 (2015)
Accepted for publication:
16 February 2015

Anterior superior alveolar nerve (ASAN)

A morphometric-anatomical analysis

KEYWORDS
anterior superior alveolar nerve,
morphology,
morphometry,
anatomy

SUMMARY

The anterior superior alveolar nerve (ASAN) is a branch of the infraorbital nerve. Only few studies have morphometrically evaluated the course of the ASAN. Midfacial segments of ten hemisectioned fresh adult cadaver heads were dissected to uncover the anterior wall of the maxilla. Specimens were subsequently decalcified and the bone overlying the ASAN was removed under a microscope to expose the ASAN. Its branching pattern from the infraorbital nerve was recorded, and the course of the ASAN within the anterior wall of the maxillary sinus was morphometrically assessed measuring distances to predefined landmarks using a digital caliper. A distinct ASAN was observed in all specimens. It arose lateral (six cases) or inferior (four cases) from the infraorbital nerve. The point of origin was located at a mean distance of 12.2 ± 5.79 mm posterior to the infraorbital foramen. The ASAN was located on average 2.8 ± 5.13 mm lateral to the infraorbital foramen. After coursing medially, the ASAN ran inferior to the foramen at a mean distance of 5.5 ± 3.07 mm. When approaching the nasal aperture, the loop of the ASAN was on average 13.6 ± 3.07 mm above the nasal floor. The horizontal mean distance from the ASAN to the nasal aperture was 4.3 ± 2.74 mm halfway down from the loop, and 3.3 ± 2.60 mm at the floor of the nose, respectively. In conclusion, the present study evaluated the course of the ASAN relative to the infraorbital foramen and nasal aperture. This information is helpful to avoid damage to this anatomical structure during interventions in the infraobrital region of the maxilla. Further, knowledge of the course of the ASAN and of its bony correlate *(canalis sinuosus)* may be valuable in interpreting anesthetic or radiologic findings in the anterior maxilla.

Introduction

The anterior superior alveolar nerve (ASAN) is a branch of the infraorbital nerve traditionally considered to contribute to the superior dental plexus together with the middle and posterior superior alveolar nerves. The ASAN is usually much thicker than the middle and posterior superior alveolar nerves, and traverses the anterior wall of the maxilla in a distinct bone canal, the so-called *canalis sinuosus*. The ASAN may consist of one to two trunks with a single branch or multiple branches (Robinson & Wormald 2005). Others have described the ASAN being made up of two to three fascicles (Murakami et al. 1994). The ASAN is usually accompanied by a small artery, the anterior superior alveolar artery. The course of the ASAN and the artery is of interest to dentists, to oral and maxillofacial surgeons, as well as to oto-rhino-laryngologists who all perform interventions and surgeries in the distribution area of these neurovascular structures.

The course of the ASAN and its bony canal (*canalis sinuosus*, Fig. 1) were first described by Wood-Jones (1939). The canal, also termed sinuous canaliculus or anterior superior alveolar canal (Song et al. 2012), originates from the infraorbital canal posterior to the infraorbital foramen and courses in an antero-lateral direction. After reaching the anterior wall of the maxilla, the *canalis sinuosus* turns medial to run below the infraorbital foramen crossing the antrum wall from lateral to medial. Once the canal reaches the nasal aperture, it loops inferiorly and descends along the piriform opening. The course of the ASAN as well as the accompanying vascular elements are inexorably bound to the *canalis sinuosus*. Yet little quantitative information concerning the course of the ASAN within the anterior wall of the maxilla is available.

The objective of the present study was to analyze and measure the trajectory of the ASAN within the anterior maxilla. The information presented here will provide greater clinical resolution concerning the location and route of the ASAN necessary for successful surgical interventions.

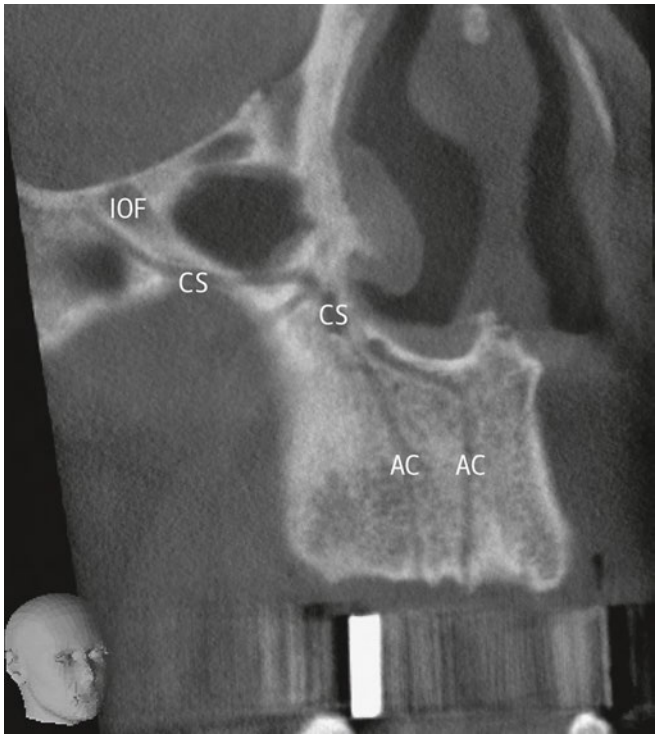

Fig. 1 Reformatted (oblique) CBCT plane through right midface/anterior maxilla of a 62-year old male showing CS and AC.

Materials and methods

The study was performed in ten midface segments of five cadaver heads. All procedures followed institutional guidelines of the Willed Body Program, University of Hawaii School of Medicine (Labrash & Lozanoff 2007). The freshly frozen cadaver heads were sectioned vertically at the anatomical midline using a bandsaw. Hemifaces were sectioned horizontally at the level of the occlusal plane and slightly above the infraorbital rim to provide midface segments. After thawing, the specimens were dissected to expose the nasal aperture, the anterior and lateral walls of the maxilla, and the orbital floor. All soft tissues covering the mentioned bone surfaces were carefully removed and the infraorbital neurovascular bundle was sectioned at the level of the infraorbital foramen. For decalcification the dissected midface specimens were put in a special solution (R.B.D. Rapid Bone Decalcifier, American MasterTech, Lodi, CA, USA) for 16 hours at room temperature. After decalcification, the specimens were thoroughly washed with tap water. The softened bone covering the ASAN was carefully removed under a microscope to visualize and measure the course of the nerve. The following morphological details were assessed: origin of ASAN relative to infraorbital nerve; and, number of trunks, fascicles and branches of ASAN. The course of the ASAN was measured relative to adjacent landmarks (infraorbital foramen, nasal aperture) including two reference lines (line A = horizontal line through upper margin of infraorbital foramen; line B = horizontal line through lower border of nasal aperture) (Tab. I and II,

Tab. I Explanation of abbreviations

Abbreviation	Anatomical correlate
AC	Accessory bone canal in anterior maxilla
AN	Anastomosis between ASAA and PSAA
ASAN	Anterior superior alveolar nerve
ASAA	Anterior superior alveolar artery
AWM	Anterior wall of maxilla
CS	Canalis sinuosus
IOA	Infraorbital artery
IOC	Infraorbital canal
IOF	Infraorbital foramen
ION	Infraorbital nerve
IOR	Infraorbital rim
MSAN	Middle superior alveolar nerve
NA	Nasal aperture
OF	Orbital floor
PSAA	Posterior superior alveolar artery
PSAN	Posterior superior alveolar nerve
SM	Schneiderian membrane

Tab. II Morphometric measurements (mm) related to ASAN and adjacent anatomical structures

# see Fig. 2	Distance	Mean ± standard deviation	Range
1	Antero-posterior distance from origin of ASAN to IOF	12.2 ± 5.79	3.04 – 19.03
2	Horizontal distance from ASAN to NA at level of line A	24.7 ± 6.56	16.68 – 36.60
3	Horizontal distance from ASAN to lateral margin of IOF	2.8 ± 5.13	-4.17* – 9.33**
4	Horizontal distance (width) of IOF	3.9 ± 0.40	3.14 – 4.62
5	Horizontal distance from medial margin of IOF to NA	17.0 ± 3.91	10.71 – 25.43
6	Vertical distance from line A to ASAN	5.5 ± 3.07	0.96 – 9.97
7	Vertical distance from line A to ASAN at midpoint between IOF and NA	8.7 ± 2.98	4.92 – 11.67
8	Vertical distance from line A to line B	23.0 ± 4.62	16.15 – 29.60
9	Horizontal distance from ASAN to NA at halfway of distance #8	5.8 ± 1.96	3.17 – 9.29
10	Vertical distance from loop of ASAN to line B	13.6 ± 3.07	8.16 – 17.36
11	Horizontal distance from ASAN to NA at halfway of distance #10	4.3 ± 2.74	0.06 – 10.03
12	Horizontal distance from ASAN to NA at level of line B	3.3 ± 2.60	0.52 – 9.65

* negative value = ASAN positioned medial to lateral margin of IOF
** positive value = ASAN positioned lateral to lateral margin of IOF

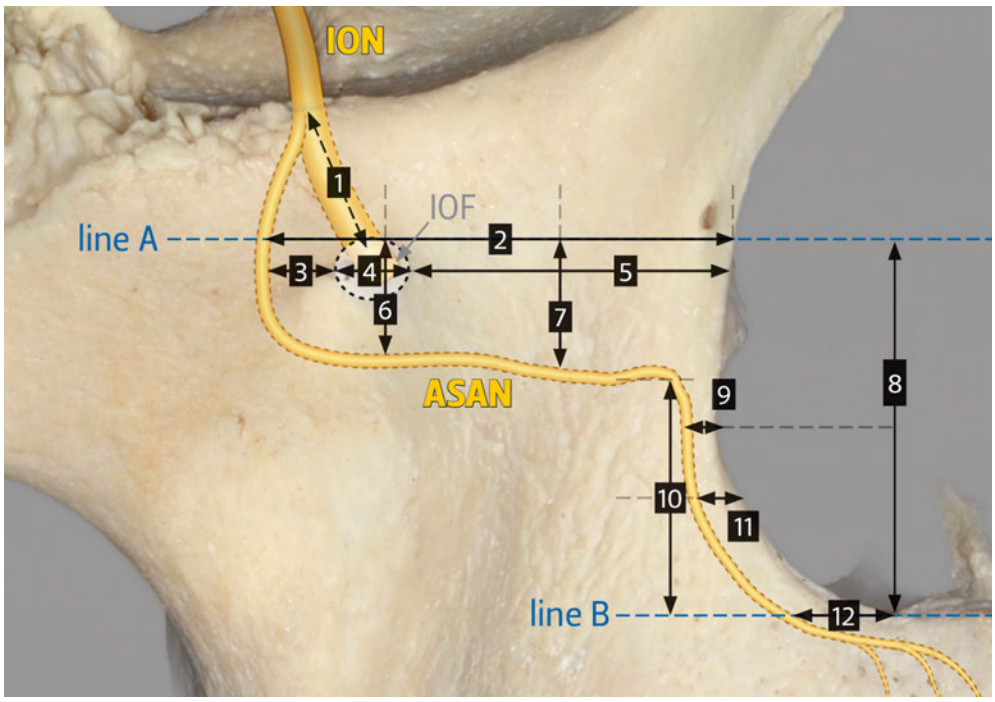

Fig. 2 Schematic illustration (not to scale) showing reference lines and measurements taken to assess the trajectory of the ASAN along the anterior wall of the maxilla.

Fig. 2). All measurements were taken with a digital caliper to the nearest .01 mm (Tresna®, Tresna Instruments, Guilin, China).

Results

Morphological findings

The ASAN could be identified in all dissected hemifaces. In all cases, it was accompanied below the orbital floor by a small artery originating from the infraorbital artery (Fig. 3). In six specimens the ASAN bifurcated laterally and in four specimens inferiorly from the infraorbital nerve (Fig. 4). All evaluated ASANs consisted of a single trunk comprising between two and four fascicles (four specimens had two fascicles, five specimens had three fascicles and one specimen presented with four fascicles). On the ventral side of the maxillary sinus, the ASAN either continued as a single branch (four specimens) or divided into two branches (four specimens), or into three branches (two specimens), respectively. The pattern with one branch curving along the nasal aperture downward to the nasal floor was found in all specimens (Fig. 5). Occasionally, an additional branch curved upward lateral to the piriform aperture, or ran inferiorly from the main trunk shortly after passing below the infraorbital foramen to join the middle or posterior superior alveolar nerves (Fig. 6). A consistent finding was an anastomosis between the anterior and posterior superior alveolar arteries (Fig. 7).

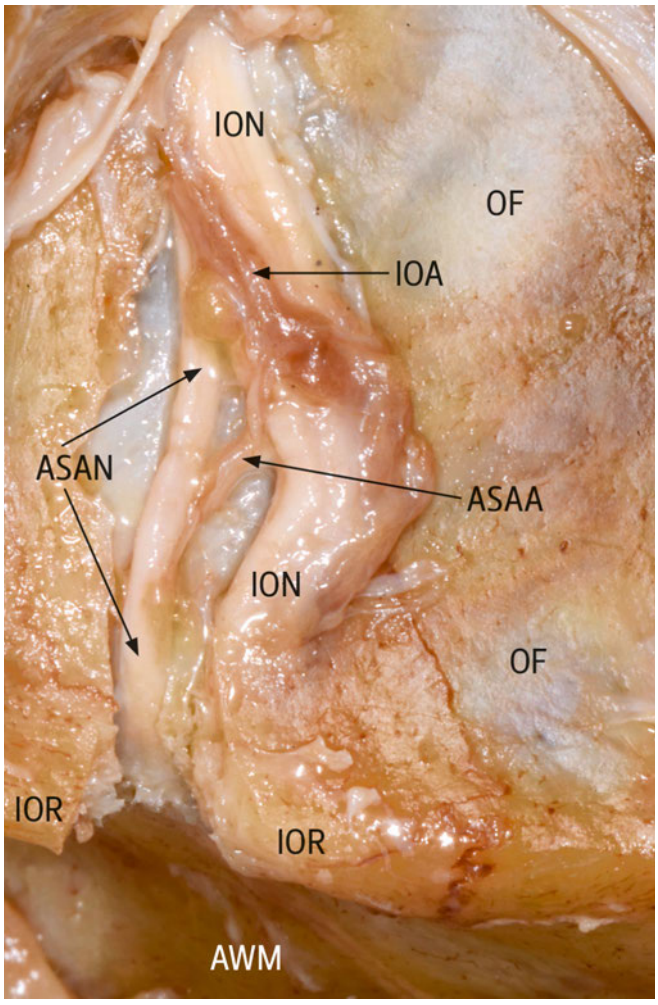

Fig. 3 Decalcified specimen: superior view of orbital floor showing origin of ASAN from ION and ASAA from IOA (part of OF and IOR have been removed to expose ASAN).

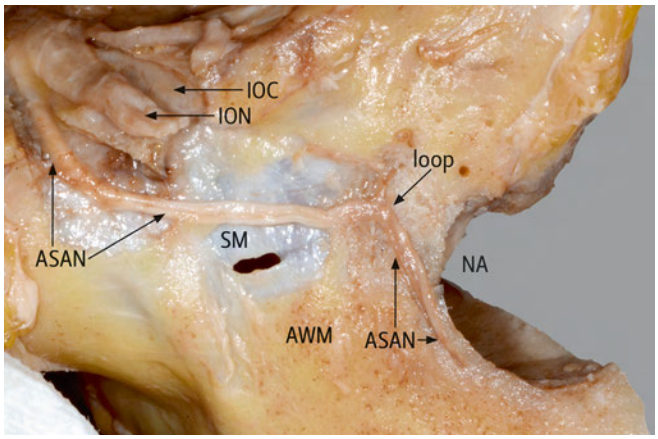

Fig. 5 Facial view of right side of decalcified specimen after removal of the thin bone covering the ASAN. The ASAN originates laterally from the ION within the infraorbital canal and shows a single trunk and single branch pattern during its course.

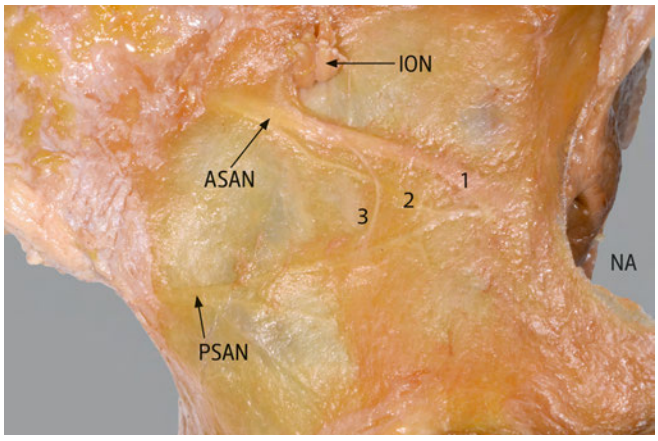

Fig. 6 Complex branching pattern of ASAN viewed anteriorly in right side of decalcified specimen. Branches #2 and #3 appear to join the forward and slightly upward running PSAN.

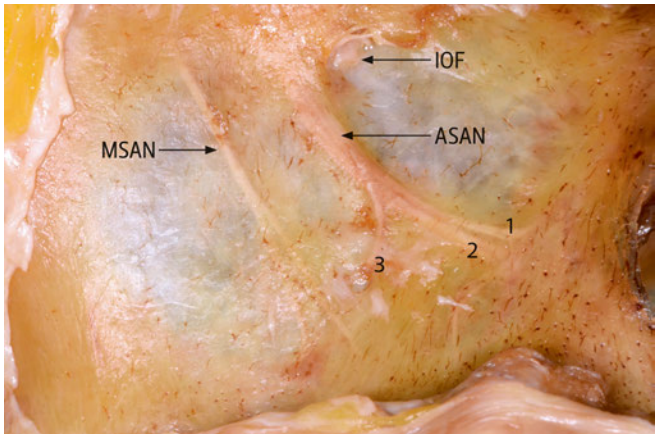

Fig. 4 Facial view of right side of midface specimen after decalcification. The ASAN emerges lateral to the IOF and ramifies into three branches within the anterior wall of the maxilla.

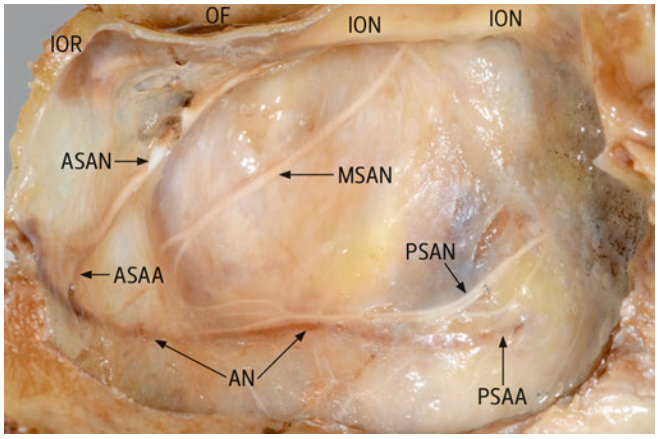

Fig. 7 Internal view of right maxillary sinus in a decalcified specimen following removal of the lateral wall of the nasal cavity but leaving the Schneiderian membrane *in situ*.

Morphometric findings (Tab. I)

The ASAN originated from the infraorbital nerve at a mean distance of 12.2 ± 5.79 mm posterior to the infraorbital foramen. Subsequently, the ASAN reached the anterior wall of the maxilla at a mean distance of 2.8 ± 5.13 mm lateral to the infraorbital foramen. However, this distance was largely dependent on the origin of the ASAN relative to the infraorbital nerve. Further along its course, the ASAN was located at a mean distance of 5.5 ± 3.07 mm below the infraorbital foramen. The loop of the ASAN approaching the nasal aperture was located at a mean distance of 13.6 ± 3.07 mm above the nasal floor. With regard to its downward course along the piriform opening, the ASAN was located at a mean distance of 4.3 ± 2.74 mm (midway between the loop and the nasal floor), and of 3.3 ± 2.60 mm (at the level

of the nasal floor), respectively, from the lateral border of the nasal aperture.

Discussion

The present cadaver study has morphologically and morphometrically assessed the ASAN and contributes to the limited information with regard to the anatomical variation of this anatomical structure. To our knowledge, this is the first study that has measured the trajectory of the ASAN relative to the infraorbital foramen and the lateral border of the nasal aperture. Those anatomical structures are easily discerned preoperatively on radiographs and are also readily visible during surgery.

Origin of ASAN

Though Heasman (1984) measured the distance between the origin of the ASAN and the infraorbital foramen he did not provide data regarding mean, minimum and maximum values for that distance. He only reported that in six specimens the distance was < 5 mm, in four specimens 5–10 mm, in five specimens 10–20 mm, and in another four specimens > 20 mm. In the present study, that distance ranged between 3.0 and 19.0 mm, but never exceeded 20 mm. A dual origin of the ASAN was never observed in the present study, but has been reported earlier (Heasman 1984, Song et al. 2012).

Morphology of ASAN

Previous observations that the diameter of the ASAN was consistently between one-half and one-third that of the infraorbital nerve and was a broader structure than either the middle or posterior superior alveolar nerves (Heasman 1984) could be visually corroborated in the present study.

Course and branching pattern of ASAN

Branching of the ASAN as observed in the present study is a common finding. Heasman (1984) described division of the ASAN into two branches in 10.5% (2/19) with the upper branch continuing to the narial margin and the lower branch joining the posterior superior alveolar nerve. In further 31.6% (6/19) the ASAN gave rise to fine branches descending and looping inferoposteriorly that finally communicated with terminal fibers of the posterior and middle superior alveolar nerves. Murakami et al. (1994) reported that the ASAN, two to three in number, arose from the infraorbital nerve after its exit from the infraorbital foramen. The ASAN divided into numerous twigs that formed the anterior part of the superior dental plexus. Robinson & Wormald (2005) described five discrete patterns to the course of the ASAN and its branches. The most common pattern was a single trunk with no branches (30%) followed by a multiple-branch pattern from a single trunk (25%). The authors observed a double trunk in 25%. In 35% of their cases, the branches of ASAN overlying the canine fossa formed a diffuse plexus. While in the present study the ASAN always presented as a single trunk, it consisted of multiple fascicles but without spacious separation.

Encasement of ASAN

In their study of 40 hemimaxillae, Robinson & Wormald (2005) identified a dehiscent ASAN in 12.5%, while the remaining 87.5% were encased in thin bone. In the present study, all ASAN were encased in thin, and occasionally very fragile, bone as they traversed the anterior wall of the maxilla. Following decalcification, the thin bone overlying the ASAN could be easily removed with tweezers.

Distance of ASAN to infraorbital foramen

Heasman (1984) reported that the vertical distance between the inferior margin of the infraorbital foramen and the ASAN varied between 2 and 9 mm (no mean value and standard deviation were provided). In the present study, this distance (measured from the superior rather than from the inferior margin of the infraorbital foramen) ranged from 0.96 to 9.97 mm, with a mean value of 5.5 ± 3.07 mm.

Course of ASAN relative to infraorbital foramen

In a cadaver study of 20 heads, Robinson & Wormald (2005) found that the ASAN emerged from its canal lateral (42.5%) and central (also 42.5%) to the infraorbital foramen, but only in 15% medial to the infraorbital foramen. In the present study, the ASAN never appeared medial to the infraorbital foramen – it emerged in 60% laterally and in 40% inferiorly to the infraorbital foramen. In a microcomputed tomography study of 28 cadaver hemimaxillae, 57.5% of ASAN canals originated laterally from the infraorbital canal, 37.5% inferiorly and only 5% medially (Song et al. 2012).

Course of ASAN relative to nasal aperture

The horizontal distance of the *canalis sinuosus* relative to the piriform aperture was assessed in 14 Korean hemifaces following decalcification and sectioning on three levels (Hwang et al. 2011). Histology was also performed with the *canalis sinuosus* containing well-defined arteries and nerves. The obtained horizontal measurements were shorter than in the present study, 0.8 mm at the bottom of the nasal aperture, 1.8 mm at a quarter and 2.6 mm at halfway of the maximum height of the nasal aperture. However, the values reported by Hwang et al. (2011) do not represent the true distance to the nasal aperture since they were taken from a reference line through the most lateral border of the nasal aperture. The safety distance of 2–3 mm stated by the authors might be too narrow to avoid the neurovascular structure along the lower half of the piriform aperture considering the mean distances measured in the present study (3.3–5.8 mm).

Clinical implications

The course of the ASAN within the infraorbital region and the anterior wall of the maxillary sinus poses for a certain risk of neurologic disorders following surgical interventions or trauma in that part of the midface. Several studies have reported changes in postoperative somatosensory function in the (anterior) maxilla after Le Fort I osteotomies (Rosenberg & Sailer 1994, Al-Din et al. 1996, Ueki et al. 2008). A study including 25 patients followed for one year reported significant sensitivity changes of the upper lip, gingiva, and teeth following Le Fort I osteotomy. Somatosensory disturbances were present in up to 64% of the evaluated patients (Thygesen et al. 2009).

Further, the ASAN may be damaged during canine fossa puncture or antrostomy (Robinson & Wormald 2005). The same authors have suggested using the bisection of a mid-pupillary line and a line through the floor of the nasal vestibule as the landmark to avoid damage to the major branches of the ASAN during canine fossa puncture. Using those described landmarks the frequency of adverse events in conjunction with canine fossa puncture could be reduced from 76% to 45%, and the number of patients complaining of persistent symptoms (facial numbness, facial tingling) was reduced from 29% to 5% (Robinson et al. 2005, Singhal et al. 2007). The same group of

authors have further demonstrated that transillumination of the maxillary sinus allows for accurate identification of the main trunk of the ASAN during canine fossa puncture (Tan et al. 2009).

Recent CBCT-based research has demonstrated bone channels in the anterior maxilla communicating with the *canalis sinuosus* (Temmerman et al. 2011, de Oliveira-Santos et al. 2013, von Arx et al. 2013). Those accessory bone channels either reach the apices of the anterior teeth or perforate the cortex on the palatal aspect of the anterior teeth (Fig. 8 and 9). We speculate that there is additional neural supply to the anterior palate via these structures, since some of the evaluated specimens showed fine neurovascular structures continuing from the piriform canal deep into the palatal alveolar bone below the anterior nasal floor. Thus, sensitivity in the anterior palate may be sustained after sectioning the nasopalatine nerve via branches from the ASAN, and not necessarily from the greater palatine nerve, as has previously been postulated (Langford et al. 1989, Filippi et al. 1999). Song et al. (2012) suggested that the lower portion of the *canalis sinuosus,* the piriform canal, reached the midline and might anastomose with the contralateral side, explaining anesthesia failure of central incisors after an infraorbital block due to cross-innervation via a contralateral ASAN branch. In addition, superimposition of the lower portion of the *canalis sinuosus* (or its continuing accessory bone channels) onto the anterior maxillary teeth may mimic intra- or periradicular lesions (Shelley et al. 1999).

In conclusion, the present cadaver study has morphometrically evaluated the course of the ASAN relative to adjacent anatomical landmarks which are readily discernible radiographically and intraoperatively, i.e. the infraorbital foramen and the nasal aperture. This information is useful to prevent neurovascular damage to the ASAN and artery during interventions in the infraorbital region of the maxilla.

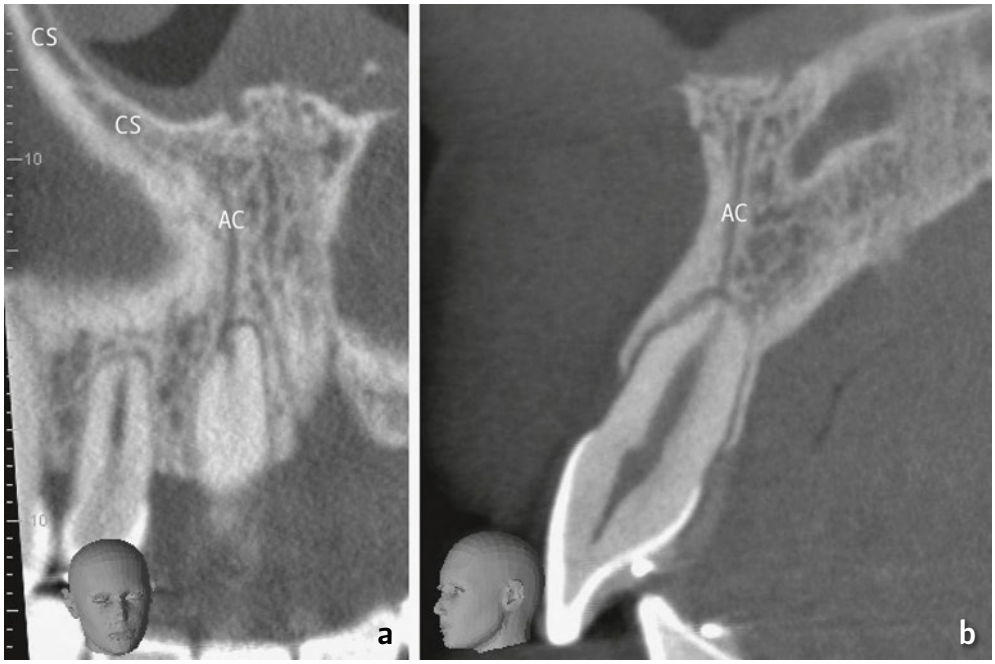

Fig. 8 Coronal (a) and sagittal (b) reformatted CBCT images of a 22-year old male showing AC (originating from CS) supplying the right central maxillary incisor.

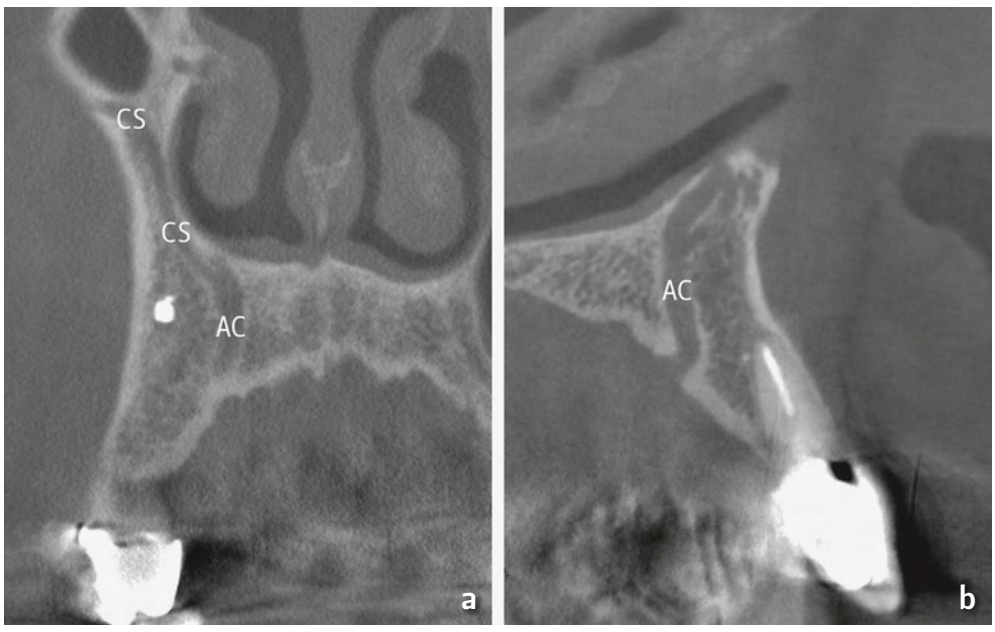

Fig. 9 Coronal (a) and sagittal (b) reformatted CBCT images of a 72-year old male showing AC (originating from CS) reaching the palate posterior to the right lateral maxillary incisor.

Acknowledgements

The authors thank Steven Labrash, Director of Willed Body Program, Department of Anatomy, Biochemistry and Physiology, John A. Burns School of Medicine, University of Hawaii, Honolulu, HI/USA, for his commitment and support. The authors also thank Ines Badertscher and Bernadette Rawyler, both form the School of Dental Medicine, University of Bern, Bern, Switzerland, for helping with the figures.

Finally, the authors wish to express their deep gratitude to the donors of the cadavers used in this anatomical study.

Résumé

Le nerf alvéolaire antéro-supérieur: une analyse morphométrique et anatomique

Le trajet du nerf alvéolaire antéro-supérieur fut décrit pour la première fois en 1939 par Wood-Jones. Le nerf alvéolaire antéro-supérieur est une branche du nerf infra-orbitaire et émerge de celui-ci dans le canal infra-orbitaire en dessous de la cavité orbitaire. Ensuite, le nerf alvéolaire antéro-supérieur se dirige vers antéro-latéral, traverse le *canalis sinuosus* dans la paroi antérieure du sinus maxillaire pour ensuite se diriger vers l'orifice piriforme. Ici, le nerf alvéolaire antéro-supérieur tourne de manière aiguë vers le bas (loop) et poursuit son trajet dans la paroi latérale de la cavité nasale vers la partie antérieure de la mâchoire supérieure. C'est dans cette région que se trouvent des ramifications du nerf vers les apex des dents antérieures, mais aussi vers la partie antérieure du palais. Peu d'études ont analysé le trajet du nerf alvéolaire antéro-supérieur du point de vue morphométrique. L'étage moyen de la face de dix semi-têtes de cadavres frais adultes a été disséqué de toutes les parties molles pour exposer la partie antérieure de l'os maxillaire. Ensuite les préparations ont été décalcifiées pour éliminer la fine couche osseuse qui recouvrait le nerf alvéolaire antéro-supérieur et pour exposer ce nerf. Le trajet et les ramifications du nerf alvéolaire antéro-supérieur dans la paroi antérieure du sinus maxillaire ont été documentés, photographiés, et des mesures avec un instrument digital ont été faites par rapport à des points de référence (foramen infra-orbitaire, orifice piriforme, etc.). Le nerf alvéolaire antéro-supérieur a pu être identifié dans toutes les préparations. L'origine de ce nerf était latérale du nerf infra-orbitaire dans six cas et caudale dans quatre cas. En moyenne, cette ramification se trouvait 12,2 ± 5,79 mm postérieur du foramen infra-orbitaire. Ensuite le nerf alvéolaire antéro-supérieure se dirigeait vers la paroi antérieure du sinus maxillaire où il passait en moyenne 2,8 ± 5,13 mm latéral du foramen infra-orbitaire. Puis, le nerf tournait vers médiale et passait en moyenne 5,5 ± 3,07 mm au-dessous du foramen infra-orbitaire pour traverser la paroi antérieure du sinus maxillaire, en direction de l'orifice piriforme. Ensuite, le nerf alvéolaire antéro-supérieur tournait de manière aiguë (ce «loop» se trouvait en moyenne 13,6 ± 3,07 mm au-dessus du plancher nasal) pour se diriger le long de l'orifice piriforme en direction caudale. L'écart moyen entre le nerf et l'orifice piriforme était de 4,3 ± 2,74 mm (mesuré à un niveau à mi-distance entre «loop» et plancher nasal) et 3,3 ± 2,60 mm (mesuré au niveau du plancher nasal). Cette étude présente des informations morphométriques qui sont importantes pour documenter le trajet du nerf alvéolaire antéro-supérieur et pour aider à éviter des dommages du nerf lors d'interventions dans la région infra-orbitaire. Ces dernières concernent essentiellement des interventions chirurgicales dans la région de la paroi antérieure du sinus maxillaire, par exemple l'ostéotomie maxillaire de Le Fort I ou l'antrotomie du sinus maxillaire (accès par la fosse canine). Dans la littérature, des troubles de sensibilité postopératoires de la gencive et des dents ont été décrits après les interventions mentionnées ci-dessus. De plus, de nouvelles études radiologiques avec la tomographie volumétrique numérisée ont documenté le trajet du *canalis sinuosus* et de ses canaux accessoires vers la mâchoire supérieure antérieure, ce qui est aussi intéressant pour le médecin-dentiste. Une sensibilité persistante d'une incisive maxillaire supérieure centrale après une anesthésie au niveau du foramen infra-orbitaire (bloc du nerf infra-orbitaire) pourrait être due à une innervation du nerf alvéolaire antéro-supérieur contralatéral. Aussi des projections radiologiques du *canalis 9sinuosus* ou de ses canaux accessoires sur les racines des canines ou incisives maxillaires peuvent être confondues avec des lésions intra- ou périradiculaires. C'est pour ces raisons que pour le praticien, il est utile de connaître le trajet du nerf alvéolaire antéro-supérieur, respectivement du *canalis sinuosus.*

Zusammenfassung

Der Nervus alveolaris superior anterior: eine morphometrisch-anatomische Analyse

Der Verlauf des *N. alveolaris superior anterior* wurde erstmals 1939 von Wood-Jones beschrieben. Der *N. alveolaris superior anterior* ist ein Ast des *N. infraorbitalis* und entspringt aus diesem noch innerhalb des *Canalis infraorbitalis* unterhalb der Augenhöhle. Danach zieht der *N. alveolaris superior anterior* nach vorne-lateral, um dann im sogenannten *Canalis sinuosus* innerhalb der Kieferhöhlenvorderwand nach medial zur *Apertura piriformis* zu ziehen. Hat er diese erreicht, biegt er scharf nach kaudal ab (loop) und zieht dann entlang der lateralen Wand der Nasenhöhle nach unten zum anterioren Oberkiefer. Dort finden sich Verzweigungen zu den Apices der Frontzähne, aber auch zum anterioren Gaumen. Nur wenige Studien haben den Verlauf des *N. alveolaris superior anterior* morphometrisch ausgewertet. Das Mittelgesicht von zehn hemisezierten, frischen Leichenköpfen von Erwachsenen wurde von allen Weichteilen freipräpariert, um die Vorderwand der Maxilla darzustellen. Anschliessend wurden die Präparate entkalkt, um die den *N. alveolaris superior anterior* bedeckende dünne Knochenschicht entfernen und den Nerven exponieren zu können. Der Verlauf und die Verzweigungen des *N. alveolaris superior anterior* innerhalb der Kieferhöhlenvorderwand wurden aufgezeichnet, fotografiert und mit einem digitalen Messinstrument morphometrisch in Bezug zu Referenzpunkten (*Foramen infraorbitale, Apertura pirifromis* etc.) bestimmt. Der Nerv konnte in allen Präparaten eindeutig identifiziert werden. In sechs Fällen hatte der *N. alveolaris superior anterior* seinen Ursprung lateral und in vier Fällen kaudal vom *N. infraorbitalis.* Diese Verzweigungsstelle befand sich durchschnittlich 12,2 ± 5,79 mm posterior vom *Foramen infraorbitale.* Der *N. alveolaris superior anterior* zog dann nach vorne zur Kieferhöhlenvorderwand, wobei er durchschnittlich 2,8 ± 5,13 mm lateral vom *Foramen infraorbitale* verlief. Danach bog der *N. alveolaris superior anterior* nach medial ab und zog durchschnittlich 5,5 ± 3,07 mm unterhalb des *Foramen infraorbitale* durch die Kieferhöhlenvorderwand zur nasalen Apertur. Dort bog der Nerv als «Loop» scharf nach kaudal ab (in einer durchschnittlichen Distanz von 13,6 ± 3,07 mm oberhalb des Nasenbodens) und zog entlang der *Apertura piriformis* nach unten. Im Mittel betrugen die Abstände zwischen Nerv und knöcherner Nasenöffnung 4,3 ± 2,74 mm (auf Niveau halbe Distanz vom Loop zum Nasenboden) und 3,3 ± 2,60 mm (auf Niveau Nasenboden). Die in dieser Studie ermittelten mor-

phometrischen Daten sind wichtig für die Dokumentation des Verlaufes des *N. alveolaris superior anterior* und hilfreich zur Vermeidung von iatrogenen Schädigungen des Nerven bei Interventionen im Infraorbitalbereich. Letztere betreffen vor allem chirurgische Eingriffe im Bereich der Kieferhöhlenvorderwand, beispielsweise Le-Fort-I-Osteotomie oder Antrotomie des *Sinus maxillaris* (Kieferhöhlenzugang via *Fossa canina*). In beiden Fällen sind in der Literatur postoperative Sensibilitätsstörungen der Gingiva und der Zähne beschrieben worden. Weiter haben neuere radiologische Studien mit der digitalen Volumentomografie den Verlauf des *Canalis sinuosus* bzw. seiner akzessorischen Kanäle zum anterioren Oberkiefer dokumentiert und sind deshalb auch für den Zahnarzt von Interesse. Eine persistierende Sensitivität eines zentralen Oberkieferinzisiven nach Leitungsanästhesie am *Foramen infraorbitale* könnte auf eine Versorgung durch den *N. alveolaris superior anterior* der Gegenseite hinweisen. Weiter können radiologische Projektionen des *Canalis sinuosus* bzw. von dessen Knochenkanälen auf die Wurzeln der Schneide- und Eckzähne intra- oder periradikuläre Läsionen vortäuschen. Kenntnisse betreffend den Verlauf des *N. alveolaris superior anterior* bzw. des *Canalis sinuosus* sind deshalb für den Praktiker von hohem Nutzen.

References

Al-Din O F, Coghlan K M, Magennis P: Sensory nerve disturbance following Le Fort I osteotomy. Int J Oral Maxillofac Surg 25: 13–19 (1996)

de Oliveira-Santos C, Rubira-Bullen I R, Monteiro S A, Leon J E, Jacobs R: Neurovascular anatomical variations in the anterior palate observed on CBCT images. Clin Oral Implants Res 24: 1044–1048 (2013)

Filippi A, Pohl Y, Tekin U: Sensory disorders after separation of the nasopalatine nerve during removal of palatal displaced canines: prospective investigation. Br J Oral Maxillofac Surg 37: 134–136 (1999)

Heasman P A: Clinical anatomy of the superior alveolar nerves. Br J Oral Maxillofac Surg 22: 439–447 (1984)

Hwang K, Kim D H, Kim D J: Anterior superior alveolar artery and horizontal maxillary osteotomy. J Craniofac Surg 22: 1819–1821 (2011)

Labrash S, Lozanoff S: Standards and guidelines for willed body donations at the John A. Burns School of Medicine. Hawaii Med J 66: 72–75 (2007)

Langford R J: The contribution of the nasopalatine nerve to sensation of the hard palate. Br J Oral Maxillofac Surg 27: 379–386 (1989)

Murakami G, Ohtsuka K, Sato I, Moriyama H, Shimada K, Tomita H: The superior alveolar nerves: their topographical relationship and distribution to the maxillary sinus in human adults. Okajimas Folia Anat Jpn 70: 319–328 (1994)

Robinson S R, Baird R, Le T, Wormald P J: The incidence of complications after canine fossa puncture performed during endoscopic sinus surgery. Am J Rhinol 19: 203–206 (2005)

Robinson S, Wormald P J: Patterns of innervation of the anterior maxilla: A cadaver study with relevance to canine fossa puncture of the maxillary sinus. Laryngoscope 115: 1785–1788 (2005)

Rosenberg A, Sailer H F: A prospective study on changes in the sensibility of the oral mucosa and the mucosa of the upper lip after Le Fort I osteotomy. J Craniomaxillofac Surg 22: 286–293 (1994)

Shelley A M, Rushton V E, Horner K: Canalis sinuosus mimicking a periapical inflammatory lesion. Brit Dent J 186: 378–379 (1999)

Singhal D, Douglas R, Robinson S, Wormald P J: The incidence of complications using new landmarks and a modified technique of canine fossa puncture. Am J Rhinol 21: 316–139 (2007)

Song W C, Kim J N, Yoo J Y, Lee J Y, Won S Y, Hu K S, Kim H J, Koh K S: Microanatomy of the infraorbital canal and its connecting canals in the maxilla using 3-D reconstruction of microcomputed tomographic images. J Craniofac Surg 23: 1184–1187 (2012)

Tan N C, Floreani S R, Robinson S, Nair S, Sunkaraneni V S, Faris C, Wormald P J: Transillumination-assisted maxillary trephination: cadaver validation of a new technique. Laryngoscope 119: 984–987 (2009)

Temmerman A, Hertelé S, Teughels W, Dekeyser C, Jacobs R, Quirynen M: Are panoramic images reliable in planning sinus augmentation procedures? Clin Oral Implants Res 22: 189–194 (2011)

Thygesen T H, Bardow A, Norholt S E, Jensen J, Svensson P: Surgical risk factors and maxillary nerve function after Le Fort I osteotomy. J Oral Maxillofac Surg 67: 528–536 (2009)

Ueki K, Hashiba Y, Marukawa K, Nakagawa K, Alam S, Yamamoto E: The evaluation of surgical factors related to recovery period of upper lip hypoaesthesia after Le Fort I osteotomy. J Craniomaxillofac Surg 36: 390–394 (2008)

von Arx T, Lozanoff S, Sendi P, Bornstein M M: Assessment of bone channels other than the nasopalatine canal in the anterior maxilla using limited cone beam computed tomography. Surg Radiol Anat 35: 783–790 (2013)

Wood-Jones F: The anterior superior alveolar nerve and vessels. J Anat 73: 583–591 (1939)